Proc.4th Int. Conf. High Level Radioactive Waste Mgmt., 2023-2032, Las Vegas, April 26-30, 1993.

SMALL-SCALE BEHAVIOR OF SINGLE GRAVITY-DRIVEN FINGERS IN AN INITIALLY DRY FRACTURE

M.J. Nicholl, R.J. Glass, and H.A. Nguyen
Geoscience Assessment and Validation Division 6115
Sandia National Laboratories
Albuquerque, NM 87185
(505) 844-0945

ABSTRACT

Experiments investigating the behavior of individual, gravity-driven fingers in an initially dry, rough-walled analog fracture are presented. Fingers were initiated from constant flow to a point source. Finger structure is described in detail; specific phenomena observed include: desaturation behind the finger-tip, variation in finger path, intermittent flow structures, finger-tip bifurcation, and formation of dendritic sub-fingers. Measurements were made of finger-tip velocity, finger width, and finger-tip length. Non-dimensional forms of the measured variables are analyzed relative to the independent parameters, flow rate and gravitational gradient.

INTRODUCTION

Nicholl et al.[1] demonstrated gravity-driven infiltration instability under full-field conditions in initially dry, rough-walled analog fractures and natural fractures in volcanic tuff similar to that found at Yucca Mountain, Nevada. Magnitude of the gravity-driven saturated flux through such fractures is given by Darcy's Law as $K_s\nabla_g$, where K_s describes saturated hydraulic conductivity and ∇_g the gravitational gradient. Instability was found to occur both at input flux (q) lower than $K_s\nabla_g$ and at the cessation of stable infiltration. A series of experiments were performed in a transparent, rough-walled analog fracture to investigate instability at the cessation of slug imbibition. Experiments were conducted by rapidly applying a measured volume of dyed water to the upper boundary of the fracture from multiple point sources, allowing excess fluid to temporarily pond in a reservoir. Finite perturbations introduced by the fluid application process were observed to damp during the initial, stable infiltration phase. Instability was observed to occur when the reservoir was exhausted and drainage began along the upper boundary. Fingers were observed to develop from significant perturbations to the front at the onset of instability. Finger width appeared to be strongly correlated to the wavelength of the associated perturbation. Finger-tip velocity was shown to exhibit functional relationships with gravitational gradient and fluid input.

The aforementioned experiments considered the gross behavior of a transient wetting front; here we focus on individual fingers. In a natural system, non-uniform application of fluid and local heterogeneity along the fracture boundary are expected. As a result, hydraulic connection between the fracture aperture and fluid source will most likely occur at discrete points. Analogous behavior was observed in preliminary experiments; a porous plate was used to supply fluid to a rough-walled, analog fracture at a rate less than $K_s\nabla_g$, fingers were observed to initiate from point connections associated with local heterogeneity along the fracture/plate boundary[1]. In the experiments reported here, an analogous boundary condition is implemented using a hypodermic needle as a point source along the fracture boundary. A metered flow rate is provided by using a syringe pump; thereby allowing systematic variation of flow into an individual finger, which is not possible under full-field conditions.

Here we present experimental results exploring the behavior of individual fingers formed by steady flow at $q < K_s\nabla_g$ in an initially dry, transparent rough-walled analog fracture. We first provide a succinct description of the experimental procedure and analog system. Flow rate (Q) and gravitational gradient (∇_g) were varied systematically to explore their effects on finger behavior. We begin reporting the experimental results by describing the dynamic behavior observed during advancement of an individual finger. These features include: desaturation behind the finger-tip, variation in spatial path, intermittent flow structures, finger-tip bifurcation, and development of dendritic sub-fingers. After the qualitative description, measurements of finger behavior are presented. Finger-tip velocity, finger width, finger-tip length, and moisture content behind the finger-tip are evaluated as dimensionless parameters. Finally, we conclude with a summary of experimental results.

EXPERIMENTAL APPROACH

An analog aperture field was used to isolate infiltration flow dynamics from the effects of aperture heterogeneity, differential wettability, and matric imbibition. The analog fracture was created by holding two plates of textured glass (30.48 x 15.24 cm) in close contact. An aluminum framed test cell with 1.9 cm thick plate glass windows was used to place the test fracture under a confining pressure (20 psi) while holding the fracture boundaries open to atmospheric pressure. The test cell was mounted on a rotating test stand (RTS) allowing inclination of the test fracture. High frequency fluorescent lamps mounted in the RTS back-light the fracture plane. Digital images of the fracture plane were acquired at 512 x 512 pixels of spatial resolution and 256 gray level resolution in the visual band. Acquisition rates of up to 30 images a second are possible. Complete details of the experimental apparatus and analog aperture field are reported in Nicholl et al.[1].

System Hydraulic Properties

The test cell has provisions to seal the side boundaries of the analog fracture and fix reservoir manifolds to the ends. The sealed analog fracture was saturated by volumetric imbibition to obtain the mean aperture (ã= 0.0213 cm). Standard deviation (std. = 0.00769 cm) and correlation length (0.07 cm) of the analog aperture field were estimated from a numerical model of the aperture field. The model was created by fitting surface profilometry data in a manner that yielded the measured mean aperture[2,3]. Saturated conductivity (K_s) was found to be consistent for Reynolds numbers from 0.27 to 5.93, exhibiting a mean value of 188 cm/minute (std. = 6 cm/minute). The parallel plate approximation yields a hydraulic aperture of 0.0196 cm (std. =0.0004 cm).

Capillary properties of the analog fracture were estimated from measurements made at the conclusion of each experiment. Capillary rise (C_r) was measured from the lower boundary along the direction of maximum ∇_g, averaged over a region unaffected by the finger. Capillary drainage height (C_d) was defined as the average length of the column of fluid within the finger that is restrained from drainage by the air entry pressure. The test fracture was of insufficient length to obtain measurements of C_d at $\nabla_g = 0.125$. Under the stated conditions, capillary forces are working against gravity; therefore $\nabla_g C_r$ and $\nabla_g C_d$ are expected to be constant. While measured mean values remained consistent, standard deviation of the capillary measurements was observed to increase significantly with decreasing ∇_g. Therefore, we assume that data collected at $\nabla_g = 1.00$ most accurately reflected capillary properties of the analog fracture (C_r: mean = 2.25 cm, std. = 0.26 cm; C_d: mean = 5.1 cm, std. = 0.76 cm).

Experimental Boundary Condition

The boundary condition for instability ($q < K_s \nabla_g$) was implemented by supplying fluid to the upper boundary from a point source consisting of a single #23 hypodermic needle. The tip of the needle was inserted approximately 1 mm into the fracture at an arbitrarily selected location prior to each trial. Fluid was supplied from a syringe pump; a diversion valve immediately upstream from the needle was used to limit turn-on surges. At the conclusion of each experiment, gravimetric methods were used to calibrate Q. Experimental fluid consisted of 1 g each of FD&C blue #1 and red #3 dyes mixed into 1 liter of de-ionized water (DI). Capillary properties of the experimental fluid were tested in glass capillary tubes and found to be consistent with those of DI.

Course of Experimentation

Experiments were performed at fracture inclinations of 0, 60, 75.5, and 82.9 degrees from vertical; corresponding to ∇_g of 1.0, 0.5, 0.25, and 0.125. At each gradient, volumetric input (Q) was varied upwards from approximately 0.025 ml/minute. This lower limit reflects the ability of the syringe pump to provide a stable flow rate. At each ∇_g, Q was increased until either finger instability made measurements impossible or Q exceeded the imbibition capacity of the analog fracture. The upper limit on Q was highly dependent on fracture inclination, ranging from 2.69 ml/minute at an inclination of 82.9 degrees from vertical ($\nabla_g = 0.125$) to 13.28 ml/minute in the vertical experiments ($\nabla_g = 1.00$). For comparison, gravity-driven saturated flow ($K_s \nabla_g$) across the full width of the analog fracture would require an input flow rate (Q) of $61\nabla_g$ ml/minute. All other system parameters were held constant. During each experiment digital images were acquired at predetermined intervals; the specific interval was varied based on the expected experimental time scale. Between experiments, the test cell was disassembled and the fracture surfaces cleaned; design of the test cell allows re-assembly in a repeatable alignment.

RESULTS AND DISCUSSION

Experimental results will be presented in two main sections. Development of the wetted structure is considered first, including qualitative descriptions of desaturation behind the finger-tip, spatial path of the finger, intermittent flow, tip bifurcation, and dendrites. Quantitative measurements of finger-tip velocity, finger width, and finger-tip length are presented in the second section, along with a first-order analysis of the data relative to the independent parameters, Q and ∇_g.

Structure of the Wetted Region

The active flow region of an individual finger supplied by steady flow to a point source extends from the fluid source to the leading edge of the finger-tip. This contrasts significantly with the behavior of fingers initiated from slug infiltration, where the active flow region is limited to the compact body of fluid that makes up the finger-tip and wetted structure behind the tip is inactive at times short with respect to evaporative redistribution[1]. In the sections that follow we describe the wetted structure of fingers initiated from constant flow to a point source, considering both typical and extreme behavior.

desaturation behind the finger-tip

Development of a typical finger is shown as Figure 1. Fluid enters the analog fracture from a point source and forms a hanging column, held to the upper boundary of the fracture by capillary forces (Figure 1a). Nicholl et al.[1] presented a first order approximation for the gradient acting on the finger-tip (∇_t):

$$\nabla_t = \nabla_g + \nabla_c \quad (1)$$

$$\nabla_c \approx (\psi_a - \psi_w)/L \quad (2)$$

where ∇_c is the capillary gradient, ψ_a the air-entry pressure, ψ_w the water entry pressure, and L describes the down-gradient distance between the air and water entry boundaries of the finger. For the air/water/glass system considered here, ψ_a is more negative than ψ_w; hence ∇_c is negative and opposes ∇_g. The capillary gradient opposing motion decreases as the hanging column lengthens. When the magnitude of ∇_g exceeds that of ∇_c, the finger-tip will begin to move as a unit[1]. If velocity of the advancing tip exceeds flux into the finger, a desaturated region develops between the tip and source (Figure 1b).

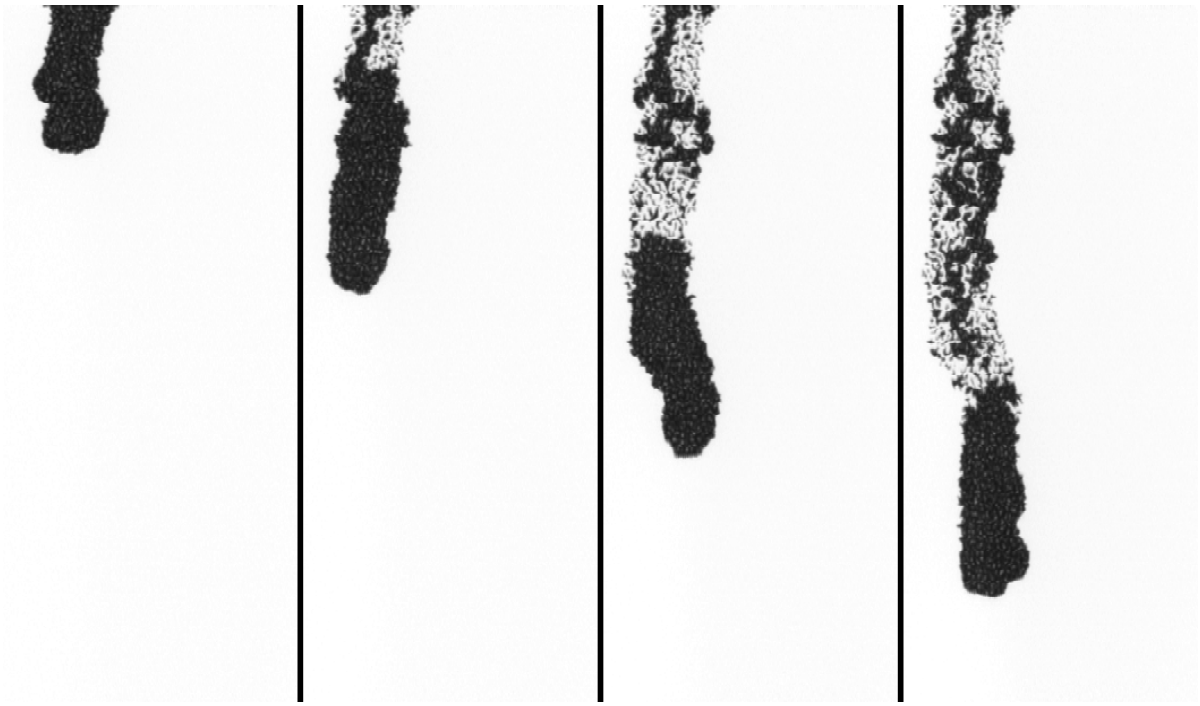

a) **b)** **c)** **d)**

Figure 1: Development of a typical finger (∇_g = 1.00, Q = 1.3615 ml/minute): a)Hanging column, time after initiation of flow (t) = 40 seconds (s); b) Desaturation behind the tip (t = 48s); c) Disconnection, note the secondary front advancing through the pre-wetted zone (t = 56s); d) The secondary front reconnects with the tip (t = 64s).

a) **b)** **c)** **d)**

Figure 2: Variation in desaturation behind the finger-tip: a) Fully disconnected (∇_g = 1.00, Q = 1.3615 ml/minute, t = 56s); b) Marginal connection (∇_g = 1.00, Q = 5.042 ml/minute, t = 16s); c) Robust connection, note the shoulder delineating the finger-tip from the drained region(∇_g = 0.50, Q = 1.344 ml/minute, t = 56s); d) Marginal drainage (∇_g = 1.00, Q = 13.283 ml/minute, t = 32s).

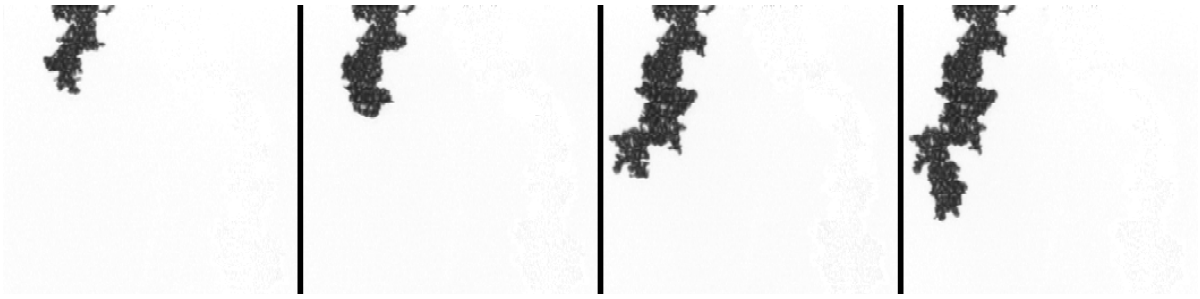

Figure 3: Spatial path of a finger (∇_g = 0.125, Q = 0.0253 ml/minute): While motion is primarily in the direction of ∇_g, local variation in capillary pressure causes the tip to wander, note the variability in tip shape as the finger responds to the local aperture field: a) t = 360s; b) t = 480s; c) t = 720s; d) t = 960s.

The structure and dynamics of the partially wetted zone behind the tip are observed to be functions of Q and ∇_g. At low flux and steep gradients, finger-tips become fully disconnected from the source (Figure 1c). Flow behind the tip also continues to advance, forming a secondary front that follows a complicated pathway through the desaturated region (Figure 1d). The secondary front was typically observed to maintain hydraulic connection with the fluid source; the special case of intermittent flow behind the tip is described in a subsequent section. Without replenishment, the finger-tip loses fluid and slows, allowing the secondary front to reconnect. Once the finger-tip is replenished it may accelerate and disconnect again, creating a quasi-periodic cycle of connection and disconnection. As Q is increased or ∇_g decreased, hydraulic connection between the source and finger-tip becomes first continuous and then increasingly robust, approaching a condition where no drainage behind the tip occurs (Figure 2). Experiments run at high flow rates and/or low gradients did not typically experience desaturation. This observation may be an artifact of the limited length of the test fracture (30.48 cm).

spatial path of the finger

The path followed by an individual finger may wander in response to local variations in fracture hydraulic properties and gradient. Finger meandering was most apparent at small values of both ∇_g and Q. Capillary pressure at the wetting front is controlled by the specific aperture field in contact with the wetting front. The narrow fingers associated with low flow rates sample only a small portion of the aperture field and are hence likely to respond to local extreme values of capillary pressure. Reducing fracture inclination increases the ratio of capillary to gravitational forces, further increasing the significance of small scale heterogeneities in determining the finger path. Figure 3 shows a finger (∇_g = 0.125, Q = 0.0253 ml/minute) meandering as it reacts to local heterogeneities in the aperture field; note the complex and dynamic shape of the fingers' leading edge. Observed finger meandering is consistent with results obtained from invasion percolation (IP) models adapted to include gravitational and surface tension effects and run under quasi-static conditions[3].

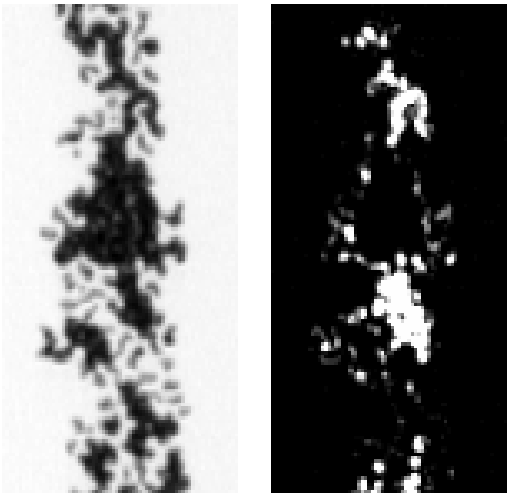

Figure 4: Intermittent flow (∇_g = 0.50, Q = 0.0251 ml/minute): a) Magnified image of a single reservoir behind the finger-tip; b) The same region with areas of repeated activity (drainage and filling) shown in white. The tendril emanating from the reservoir is a repetitive, transitory feature.

intermittent flow

At very low flow rates, the secondary front providing support to the advancing finger-tip was observed to exhibit intermittent behavior. Fluid in the desaturated region is concentrated in a string of small reservoirs, held in place by local capillary forces and separated by drained regions. A magnified image of a single reservoir is shown as Figure 4a.

Data acquisition software was written to acquire images rapidly, recording only spatial changes in the spanned aperture. Regions of repeated activity are assigned high values and stable regions low values. Dynamic behavior of the flow field shown in Figure 4a is illustrated in Figure 4b. The bright areas indicate regions where the aperture was repeatedly drained and re-filled. Areas of little change including the dry region, are black. The reservoir itself is dark, indicating that it remained filled at all times. However, immediately above and below the reservoir, the flow structure is bright, showing that these regions

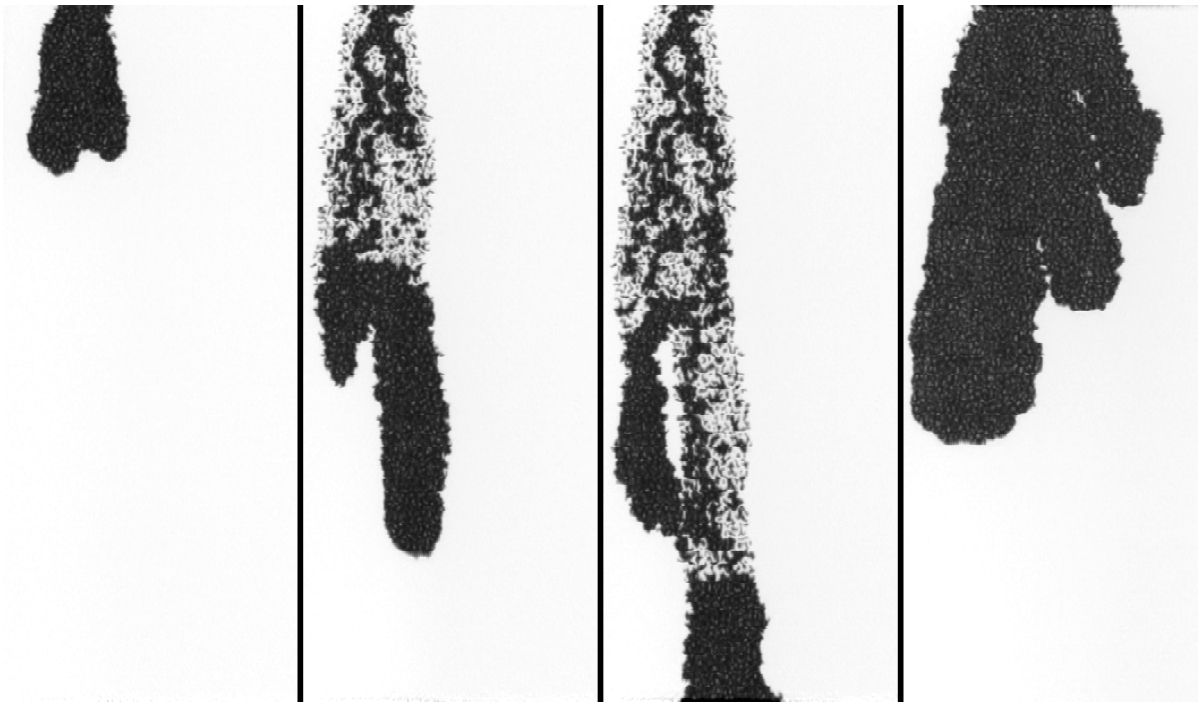

a) **b)** **c)** **d)**

Figure 5: Tip bifurcation: a) ∇_g = 1.000, Q = 2.515 ml/minute, t = 32s; b) t = 40s; c) t = 56s; d) ∇_g = 0.50, Q = 5.422 ml/minute, t = 56s.

repeatedly drain and fill. This dynamic analysis shows that hydraulic connection in the system is intermittent.

This analysis demonstrates that under certain conditions fluid moves from the source to the finger tip in discrete packets. The small reservoirs appear to absorb fluid until a critical volume is reached and then release it to flow downstream. This behavior is analogous to a series of coupled dripping faucets and may exhibit chaotic behavior. We are currently developing an experimental methodology to further explore the dynamic behavior described in this section.

tip bifurcation

The advancing tip is also subject to non-local variations in the form of unstable bifurcations. At each experimental gradient, fingers run at high flow rates were regularly observed to undergo tip splitting bifurcations (Figure 5a). In all cases, one finger dominated after the bifurcation while the other was starved of fluid and developed into a lobe on the side of the primary finger (Figure 5b). In one experiment, the finger bifurcated repeatedly within the experimental fracture (Figure 5d). Time (or distance) between events appeared to be that required for the primary finger to re-establish dominance.

Observed behavior is similar to that reported in the literature on viscous instability (see reviews[4,5,6]). Simplistic analytic solutions and numerical experimentation have provided a conceptual understanding of tip bifurcation in viscous-driven fingers. Bensimon[7] showed that surface tension serves to stabilize viscous fingers with respect to infinitesimal perturbations. However, the same analysis showed that stability with respect to finite amplitude perturbations decreases exponentially with increasing finger-tip velocity. The aperture variation characteristic of rough-walled fractures would serve as finite amplitude perturbations to an advancing finger-tip. Incidence of observed tip bifurcation increased with increasing tip velocity, as expected from analogy to Bensimons' results. Finite disturbances along the front are rapidly advected away from the tip onto the side of the finger where the rate of growth decreases (Figure 5a,b). This observed behavior is consistent with the stabilizing mechanism reported by Tabeling et al.[8] for viscous fingers.

dendrites

A second form of macroscopic structural feature observed during experimental trials were dendritic sub-fingers initiating from the sides of the primary finger. Dendrites were observed to form in approximately 35% of the experimental fingers. In most cases, formation occurred after the system had been spanned. While dendrites were observed at all flow rates and gradients, they were most prevalent in vertical experiments using either very low or high flow rates. Dendrites often initiated from the lobes associated with failed bifurcations, as illustrated in Figures 5a-c. After the initial tip bifurcation seen in Figure 5a, the left hand sub-finger slowed and developed into a lobe on the main finger (Figure 5b). The lobe did not advance further until the main finger spanned the test fracture; subsequently it resumed movement, forming a dendritic sub-finger (Figure 5c).

Pressure change within the wetted region due to contact with the fracture boundary and time dependent changes in contact angle at potential initiation sites are potential mechanisms for dendrite formation. Further investigation will require different length and/or time scales than used in these experiments and is reserved for future study.

Quantitative Measurements

A total of 80 experiments were performed, 42 at ∇_g = 1.00, 24 at ∇_g= 0.500, 8 at ∇_g = 0.250, and 6 at ∇_g = 0.125. Digital images acquired during each experiment were used to delineate temporal development of the wetted structure. Measurements of finger velocity, finger width, and finger-tip length were obtained from the data. The effects of ∇_g and Q on finger behavior are illustrated qualitatively in Figures 6 and 7, respectively. Decreasing ∇_g apparently leads to a decrease in finger velocity, along with increases in finger width, finger-tip length, and structural complexity (Figure 6). Increasing Q appears to result in increased finger velocity, width, finger-tip length, and hydraulic connection to the source (Figure 7). In the following sections we provide a quantitative analysis of the effects of ∇_g and Q on finger behavior.

finger-tip velocity

Finger-tip velocity (v) is defined as the rate of change in position of the leading edge of the finger-tip in the direction of maximum gravitational gradient. Fingers formed at the cessation of slug infiltration in a similar analog fracture were observed to exhibit both a general trend towards deceleration within the fracture and local fluctuations[1]. The deceleration was due to a loss of fluid as the tip advanced, a situation not present in these constant flow experiments. In the experiments reported here, the effects of local fluctuations were minimized by measuring velocity over the largest spatial domain possible as defined by the available images for the individual finger. Measured tip velocity exhibits definite functional relationships with both ∇_g and Q (Figure 8). Data plots on a series of four similar curves; each curve corresponds to an experimental ∇_g. As Q increases, velocity rises sharply at first and then levels off as it approaches an apparent asymptotic limit.

The relationship between tip velocity and fluid input is explored in terms of dimensionless variables, velocity ratio (R_v) and flux ratio (R_q). Division of volumetric input by mean finger width and mean fracture aperture allows fluid input to be expressed as a flux (q). Saturated velocity ($K_s\nabla_g$) provides a characteristic measure of flow velocity that may be used to non-dimensionalize both flux and velocity, as shown in equations 3 and 4.

$$R_v = v/(K_s\nabla_g) \quad (3)$$

$$R_q = q/(K_s\nabla_g) \quad (4)$$

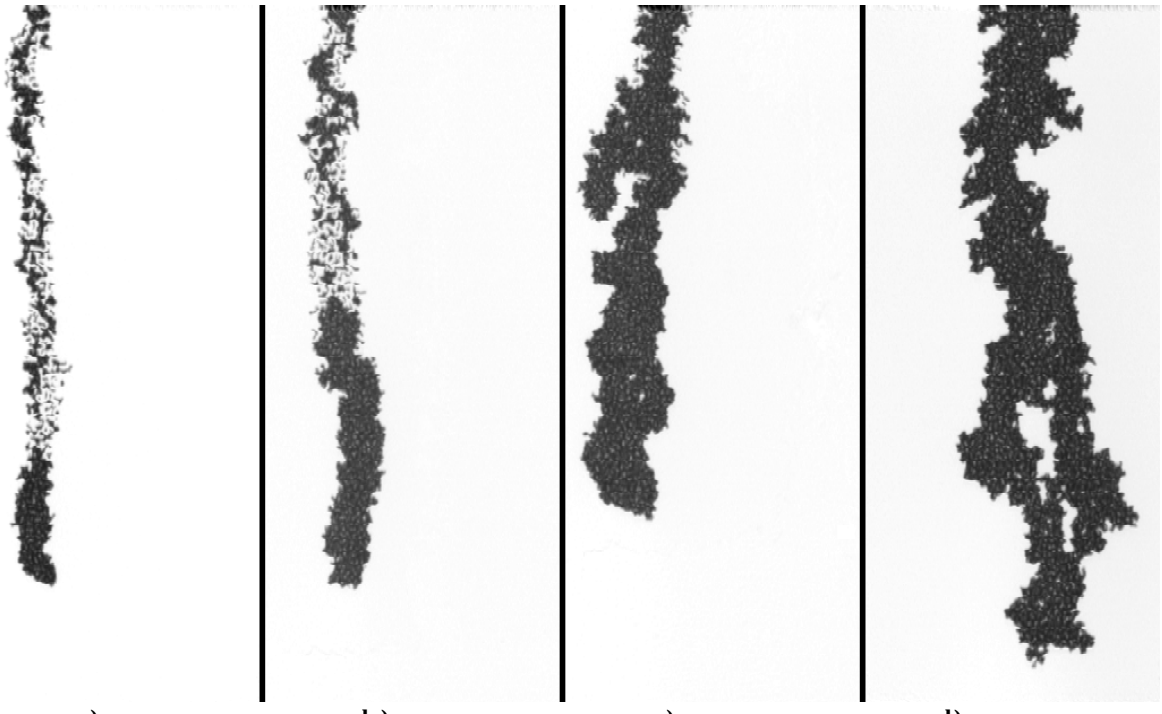

a) **b)** **c)** **d)**

Figure 6: Effects of ∇_g on finger behavior: The small differences in volumetric input have a lower order effect on finger behavior than does ∇_g: a) ∇_g = 1.000, Q = 0.2538 ml/minute, t = 99s; b) ∇_g = 0.50, Q = 0.2722 ml/minute, t = 150s; c) ∇_g = 0.25, Q = 0.2469 ml/minute, t = 285s; d) ∇_g = 0.125, Q = 0.2348 ml/minute, t = 450s.

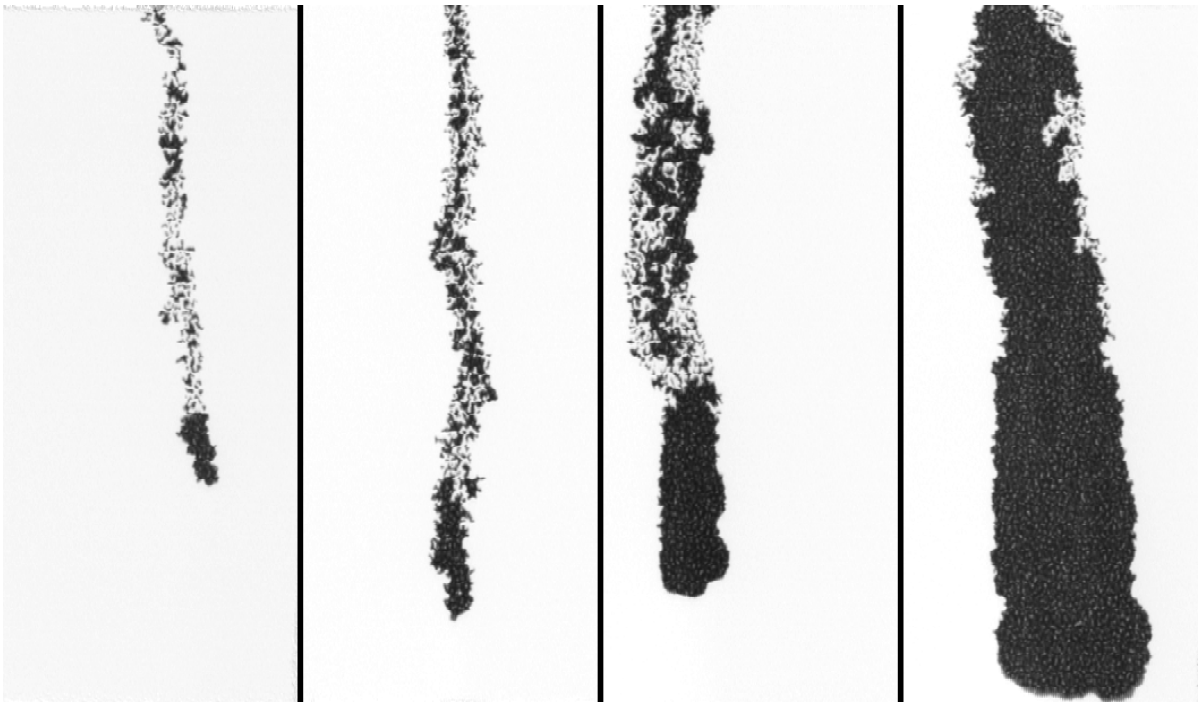

a) **b)** **c)** **d)**

Figure 7: Effects of volumetric input on finger behavior (∇_g = 1.00): a) Q = 0.0255 ml/minute, t = 150s; b) Q = 0.2584 ml/minute, t = 45s; c) Q = 1.3615 ml/minute, t = 27s; d) Q = 13.283 ml/minute, t = 8s.

Transformed data is shown as Figure 9; data is seen to collapse significantly towards a single curve. However, variation due to ∇_g is not entirely accounted for; close examination reveals that R_v increases slightly with ∇_g. Re-scaling of both dependent and independent variables by ∇_g retains non-dimensionality, and serves to collapse the data further towards a single functional form, irrespective of ∇_g (Figure 10). We are currently working towards a physically based explanation of this apparent functional form for finger-tip velocity.

The 1:1 lines in Figures 9 and 10 reflect a condition where dimensionless flux and velocity are equal. In the homogeneous analog fracture, a stable finger-tip exhibiting constant width and velocity that does not experience desaturation behind the tip is expected to plot along the 1:1 line. If desaturation occurs behind a stable tip, then velocity must exceed flux, placing data above the 1:1 line. Four data points plot significantly below the 1:1, line indicating either measurement error or that the tip had not attained steady-state. Three of the four suspect data points were collected from fingers observed to bifurcate, implying tip instability.

finger width

The domain of an individual finger is primarily delimited by the region swept by the advancing tip. Finger width (W_f) was defined as the average width of this domain, measured perpendicular to ∇_g over a region free from boundary effects and dynamic structural features (dendrites and bifurcations). Finger width is observed to increase with Q and decrease with ∇_g (Figure 11). The data also implies a unique minimum width for each ∇_g investigated. Data may be put into dimensionless form using the following relationships:

$$R_w = W_f/S_w \quad (5)$$

$$R_i = Q/(\tilde{a}K_s\nabla_g S_w) \quad (6)$$

where S_w is the width of the analog fracture. The width ratio (R_w) describes the portion of the fracture width occupied by the finger, while R_i expresses volumetric input relative to volumetric flow through the analog fracture under saturated conditions ($61\nabla_g$). The re-scaled data (Figure 12) shows a separation in flow regime with increasing R_i that was not apparent in the raw data. With one exception, fingers to the left of the vertical dashed line were observed to fully disconnect from the fluid source, while those to the right showed a mixed transition from disconnected to fully filled as R_i increased. Although there is significant scatter in the data, it does appear to collapse towards a single functional form. In the region where disconnection was prevalent, the curve rises steeply from an apparent minimum value. The curve has a slope break near or at the change in flow regime and continues to rise in an apparent linear trend. Again a physical explanation of observed behavior is under development.

finger-tip length

As previously discussed, an advancing finger is commonly seen to divide into two regions, the advancing tip and a desaturated region through which fluid is transferred to the trailing edge (tail) of the tip (Figure 2). The leading edge and

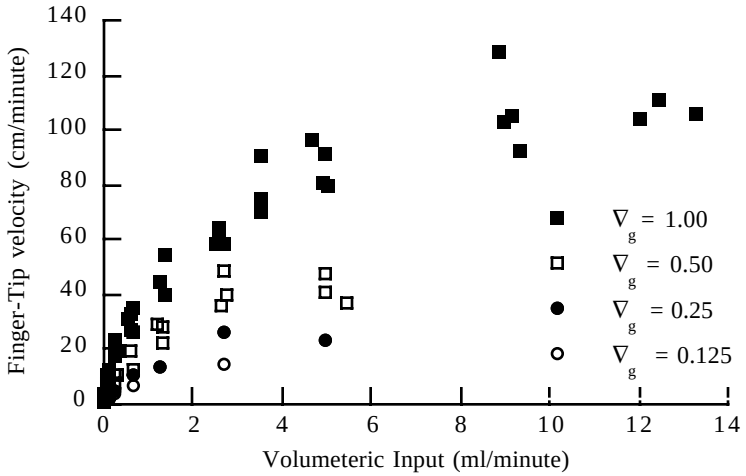

Figure 8: Finger-tip velocity as a function of volumetric input: Raw experimental data plots on four distinct curves; one for each experimental gradient. Velocity is seen to increase with both volumetric input and ∇_g.

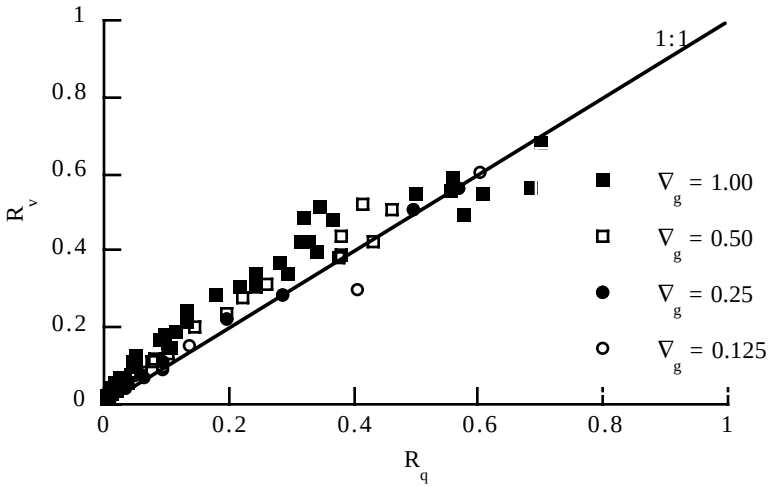

Figure 9: Dimensionless velocity (R_V) as a function of dimensionless flux (R_q): Data collapses significantly towards a single curve; however, close inspection reveals that four distinct curves exist, indicating an increase in R_V with ∇_g. The 1:1 line reflects a condition where flux and velocity are equal.

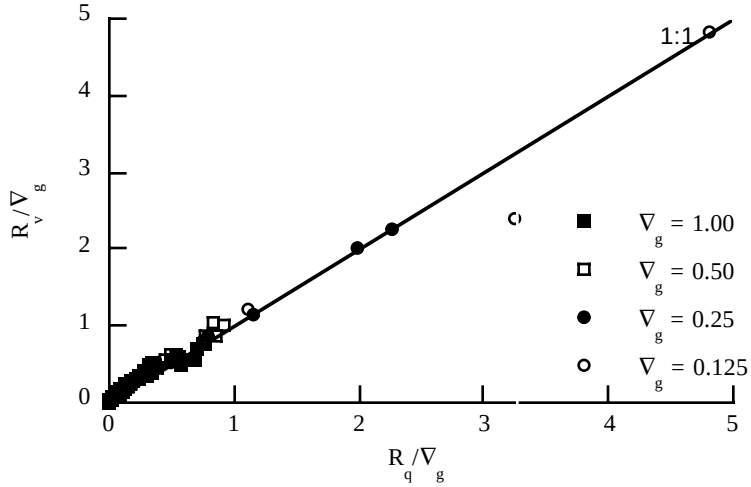

Figure 10: Dimensionless velocity and flux scaled by ∇_g: Data collapses onto a single curve.

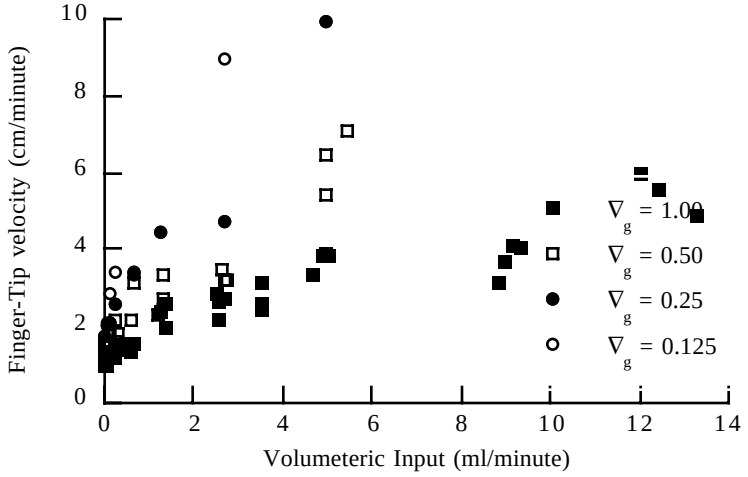

Figure 11: Finger width as a function of volumetric input: Raw experimental data plots on four distinct curves; one for each ∇_g. Each curve appears to indicate a different minimum width as Q approaches zero.

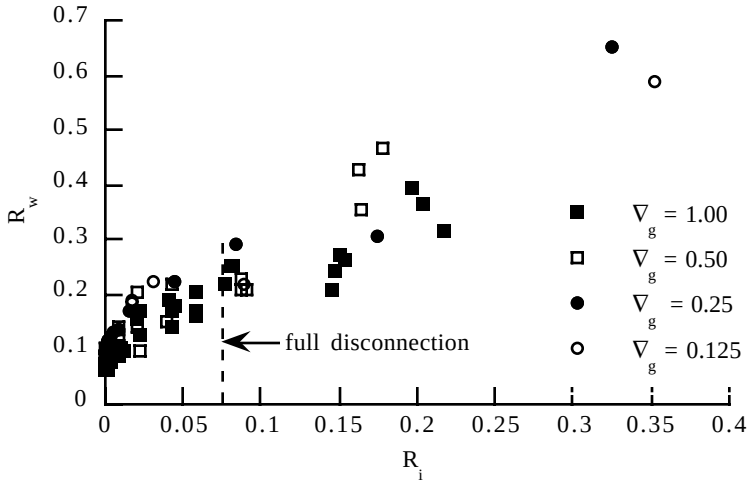

Figure 12: Dimensionless width (R_w) as a function of dimensionless flow (R_i): While data appears to collapse towards a single curve, significant scatter exists. All but one of the points to the left of the vertical line comes from a finger that was observed to fully disconnect from the fluid source.

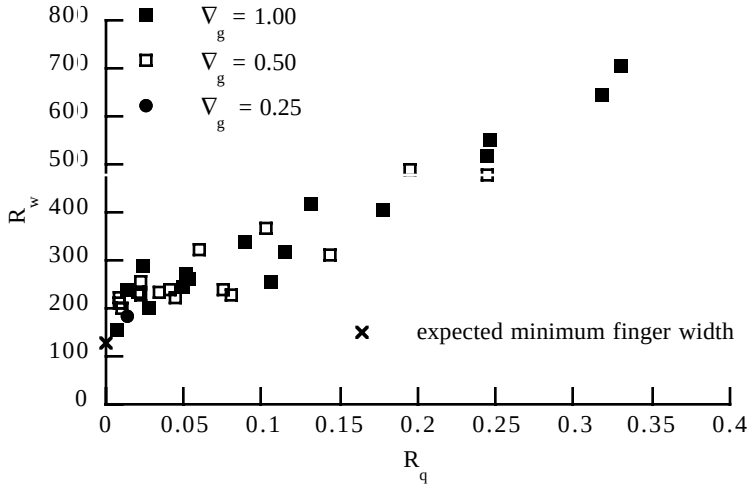

Figure 13: Dimensionless tip length as a function of dimensionless flux: R_L shows an apparent linear relationship with R_q. Data appears to indicate a minimum tip length characteristic of the fracture.

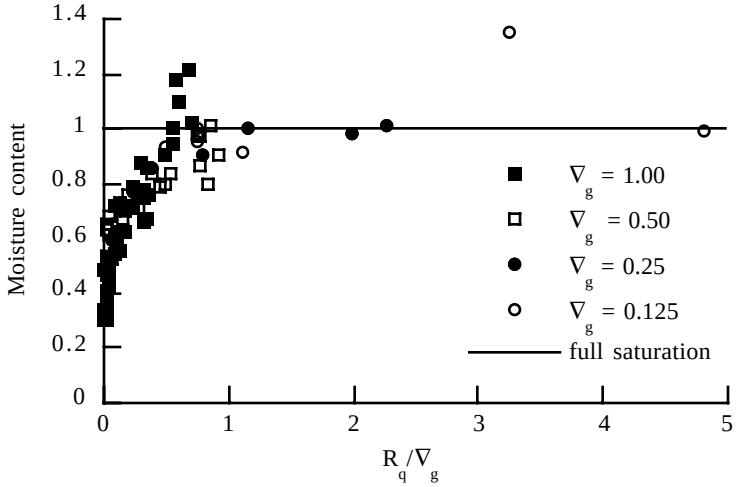

Figure 14: Moisture content as a function of dimensionless flux scaled by ∇_g: Data appears to plot along a single curve, asymptotically approaching field capacity as R_q/∇_g goes to zero and rapidly climbing towards saturation as R_q/∇_g increases.

tail of the finger-tip can best be defined as those points furthest down-gradient that are actively experiencing filling and drainage, respectively. Spatial location of the leading edge can be measured as the point furthest down-gradient where the fracture aperture is fully spanned. The structure along the trailing edge is considerably more complicated than the leading edge, making it difficult to specify a single point on a digital image as undergoing active drainage. For fully disconnected fingers, the tail was defined by visually locating the average line of active desaturation (Figure 2a). Fingers that desaturate behind the tip, but remain connected to the fluid source exhibit a transition region where flow from the source connects with the advancing finger-tip (Figures 2b,c). On such fingers, spatial location of the tail was arbitrarily located by visually fitting a line perpendicular to ∇_g through the transition zone. Tip length (L_t) was defined as the down-gradient distance between the tip and tail of the finger. Because no desaturation occurred in experiments at high flow and/or low gradient a limited number of measurements were possible (26 at ∇_g = 1.00, 16 at ∇_g= 0.500, 1 at ∇_g = 0.250, and 0 at ∇_g = 0.125).

Capillary gradient within the finger-tip is expected to vary with tip length (equation 2). Assuming that $_a$ and $_w$ are constant; the ratio of capillary to gravitational forces will vary as the inverse of $L_t\nabla_g$. Mean aperture, a characteristic length associated with capillary properties of the analog fracture is used to express L_t in dimensionless form as a length ratio (R_L).

$$R_L = L_t\nabla_g/\tilde{a} \qquad (7)$$

Available measurements are shown in Figure 13 as a function of R_q. The data seems to display a linear relationship except at low values of R_q, where the functional form appears to differ. First order theory[1] implies the existence of a minimum tip length, below which movement is not expected to occur. Assuming that C_d and C_r provide appropriate measures of ψ_a and ψ_w, equations 1 and 2 may be used to estimate R_L at R_q = 0. The estimated value of 127 differs from the apparent linear trend observed in Figure 13. This discrepancy may be an artifact of the measurement process; measurement of L_t may have been systematically biased by differences in the characteristic shape of the wetting and drying fronts. In addition, measured C_d and C_r may have included boundary effects that invalidate the measurement as an estimator of ψ_a and ψ_w. An alternative explanation could be found in assessing the influence of dynamic variation in contact angle. We reserve resolution of this discrepancy for future experimentation on the dynamic behavior of contact angle.

moisture content behind the finger-tip

The zone behind an advancing finger-tip acts as a support structure, carrying fluid to the tip; saturation within this zone may range from 100% to near field capacity. Moisture content within a fracture may be defined as the percentage of the aperture volume that is fluid filled. If the finger-tip is advancing at constant velocity and width through the homogeneous analog fracture, then the aperture volume swept by the finger-tip ($v\tilde{a}W_f$) should also be constant. Assuming that the finger-tip has achieved steady-state implies that the finger shape and tip length are also constant. Flow into the finger (Q) must then act solely to extend the support structure at the same velocity as the tip. Moisture content of the support structure (M_c) may therefore be defined as follows:

$$M_c = Q/(v\tilde{a}W_f) \cdot 100\% \qquad (8)$$

Moisture content is shown as a function of R_q/∇_g in Figure 14. Data appears to plot along a single curve, rising quickly from approximately 30% to saturation (100%). As experiments were conducted with constant flow into the finger, moisture content of the support structure associated with a stable, steady-state finger-tip is expected to exceed field capacity. Therefore, actual field capacity is expected to be smaller than the lowest observed data value (30%). Experimental data that appear to indicate an unphysical situation (M_c > 100%) result for the same reasons as the data that plots below the 1:1 line in Figures 9 and 10. Equation 8 is based on an assumption of steady-state behavior. As previously discussed, these discrepancies are believed to result from either measurement error or non-steady-state behavior as discussed in previous sections on intermittent flow and tip bifurcation.

CONCLUSIONS

Individual fingers initiated from a point source are typically observed to separate into two regions, a finger-tip that advances down-gradient as a coherent body and a partially drained region between the finger-tip and the source. Drainage behind the tip was not observed at low ∇_g and/or high Q, most likely due to the limited length of the experimental fracture. As fracture inclination is decreased, the ratio of capillary to gravitational forces increases; fingers are observed to become slower, wider, and wander more. Increasing volumetric input leads to increased velocity and increased connection between the finger-tip and fluid source. Large finger-tip velocity is observed to lead to tip instability, manifested as tip bifurcation. At low flow rates intermittent flow structures are observed in the desaturated region behind the tip. Dendritic sub-fingers were observed to preferentially occur after flow spanned the experimental fracture. The independent parameters, ∇_g and Q may be combined in dimensionless form as either a flux ratio (R_q), or flow ratio (R_i). Flux ratio is defined as flux through the finger relative to gravitationally driven saturated flux, while flow ratio describes volumetric flow into the finger relative to saturated flow through the full fracture width. Dimensionless finger-tip velocity, length, and moisture content display functional relationships with the flux ratio. Dimensionless finger width displays a functional relationship with flow ratio. Future work will consider physically based explanations for these apparent functional forms.

These results provide an additional step towards development of adequate conceptual models of flow through unsaturated fractures. Previous work by Nicholl et al.[1] explored boundary conditions leading to gravity-driven infiltration flow instability and provided a first-order explanation of wetting front behavior at the cessation of full-field slug infiltration

into an initially dry analog fracture. Work also published in these proceedings[9], considers the effects of initial moisture fields on both slug infiltration and constant flow from a point source. Future work will consider the effects of aperture heterogeneity and matric imbibition on finger behavior. Development of pore-scale models capable of capturing the dynamics of wetting front instability is underway[3]. When completed, this body of work will provide a basis for the inclusion of gravity-driven instability into both conceptual and numerical models of flow through unsaturated fractured rock.

ACKNOWLEDGMENTS

The authors gratefully acknowledge the assistance and support of W.C. Ginn in design and fabrication of the experimental apparatus and L. Orear in development of image acquisition software. This work was supported by the U.S. Department of Energy, Office of Civilian Radioactive Waste Management, Yucca Mountain Site Characterization Project Office, under contract DE-AC04-76DP00789.

REFERENCES

1. M.J. NICHOLL, R.J. GLASS, and H.A. NGUYEN, "Gravity-Driven Fingering in Unsaturated Fractures", Proceedings of the Third Annual International Conference on High Level Radioactive Waste Conference, Las Vegas, Nevada, April 12-16, (1992).

2. R.J. GLASS, M.J. NICHOLL, and M.E. THOMPSON, "Comparison of Measured and Calculated Permeability for a Saturated, Rough-Walled Fracture", Presented at the Fall 1991 AGU Meeting, (H51D-11) EOS, 72, 216, (1991).

3. R.J. GLASS, "Modeling Gravity-Driven Fingering Using Modified Percolation Theory", Proceedings of the Fourth Annual International Conference on High Level Radioactive Waste Conference, Las Vegas, Nevada, April 26-30, (1993).

4. D.BENSIMON, L.P. KADANOFF, S. LIANG, B.I. SHRAIMAN, C. TANG, "Viscous Flows in Two Dimensions", Reviews in Modern Physics, vol. 58, no. 4, pp. 977-99, (1986).

5. G.M. HOMSY, "Viscous Fingering in Porous Media", Ann. Rev. Fluid Mech., 19, 271-311 (1987).

6. P.G. SAFFMAN, "Viscous Fingering in Hele-Shaw Cells", J. Fl. Mech., 173, 73 (1986).

7. D. BENSIMON, "Stability of Viscous Fingering", Phys. Rev. A, vol. 33, no. 2, pp. 1302-8, (1986).

8. P. TABELING, G. ZOCCHI, and A. LIBCHABER, "An Experimental Study of the Saffman-Taylor Instability", J. Fl. Mech., vol. 177, pp67-82, (1987).

9. M.J. NICHOLL, R.J. GLASS, and H.A. NGUYEN, "Wetting Front Instability in an Initially Wet Unsaturated Fracture", Proceedings of the Fourth Annual International Conference on High Level Radioactive Waste Conference, Las Vegas, Nevada, April 26-30, (1993).